RSC Advances

PAPER

View Article Online
View Journal | View Issue

Check for updates

Cite this: *RSC Adv.*, 2021, **11**, 37904

Formation mechanism of zigzag patterned P(NIPAM-*co*-AA)/CuS composite microspheres by *in situ* biomimetic mineralization for morphology modulation

Juxiang Yang, *[a] Daodao Hu, *[b] Wei Li,[b] Yuan Jia[a] and Pengna Li[a]

Poly(*N*-isopropylacrylamide-*co*-acrylic acid)/copper sulfide (P(NIPAM-*co*-AA)/CuS) composite microspheres with variable zigzag patterned surfaces have been synthesized by employing an *in situ* biomimetic mineralization reaction between H_2S and Cu^{2+} immersed in P(NIPAM-*co*-AA) microspheres for morphology modulation. The morphology and composition of the P(NIPAM-*co*-AA)/CuS composite microspheres with zigzag patterned surfaces prepared in different conditions were characterized by scanning electron microscopy (SEM) and Fourier transform infrared spectrometry (FT-IR). The polymeric microgels swelled by $Cu(Ac)_2$ solution after freeze-drying treatment were of porous structure, indicating that there were polymeric frameworks and rich-water domains in the microgels before the deposition. Furthermore, due to the limited uneven deposition of metal sulfide on the polymeric skeleton of the hydrogel surface, the surface polymeric skeleton will be anisotropically shrunk when the composite microspheres lose water and shrink, thus forming a wrinkle pattern on the surface of the composite microspheres. The factors affecting the deposition amount and distribution of metal sulfide will affect the zigzag patterned morphology. Based on the experimental results, a formation mechanism of the P(NIPAM-*co*-AA)/CuS composite microspheres with zigzag patterned surface, "the deformed shrinkage of the surface texture", has been proposed. The formation mechanism of the surface morphology in the composite microspheres is helpful for understanding and controlling the process of mineralization, for preparing materials expected by controlling the experiment conditions, and for expanding the application of the composites.

Received 23rd June 2021
Accepted 27th October 2021

DOI: 10.1039/d1ra04872d

rsc.li/rsc-advances

Open Access Article. Published on 24 November 2021. Downloaded on 2/10/2026 2:57:07 PM.
This article is licensed under a Creative Commons Attribution-NonCommercial 3.0 Unported Licence.

1. Introduction

By bio-inspired mineralization, the design and fabrication of inorganic–organic composites with exceptional mechanical properties have been extensively studied in material research due to their potential wide-ranging applications, including chemistry, biology, and material science.[1,2] At present, it is generally believed that the process of biomineralization is carried out in the system of a near gel state. More and more biological evidences show that the organic macromolecules in organisms, such as proteins and polysaccharides, can influence the mineralization process through a supramolecular assembly to form a gel-like matrix network. For example, it has been found that protein hydrogels and many biological minerals, such as tooth enamel, pearlescent coating on shellfish, and fish otolith, are related to the main components of organic substrates.[3] Moreover, hydrogels can mediate biomineralization, which enables a variety of biological minerals to form a variety of forms in nature and has specific biological functions. Therefore, research on biomimetic mineralization based on hydrogel substrates has recently received wide attention. Furthermore, the study of bio-inspired mineralization processes using gel as a substrate has great significance in understanding the biomineralization mechanism, and guides the design and synthesis of advanced functional materials. The research is mainly to regulate the structure, morphology and orientation of the crystal by optimizing the structure and chemical properties of the template, but there are few studies to modulate the morphology by external condition.

The hydrogel matrix offers the possibility of producing hybrid materials on the macroscopic scale through the mineralization of pores within swollen networks. All of these, the interaction of the crystals with the hydrogel, the inhibition convection and the slowed diffusion of reactants, play vital roles during the process of crystallization. Until now, different kinds of natural and synthetic macromolecule gels, supermolecule hydrogels, and inorganic gels, are suitable for growing crystals

[a]*School of Chemistry and Chemical Engineering, Xi'an University, Xi'an 710065, P. R. China. E-mail: jxyang05@xawl.edu.cn; Fax: +86-29-81530702; Tel: +86-29-81530717*
[b]*School of Materials Science and Engineering, Shaanxi Normal University, Xi'an 710062, P. R. China. E-mail: daodaohu@snnu.edu.cn*

© 2021 The Author(s). Published by the Royal Society of Chemistry

Open Access Article. Published on 24 November 2021. Downloaded on 2/10/2026 2:57:07 PM.
This article is licensed under a Creative Commons Attribution-NonCommercial 3.0 Unported Licence.

within by the bio-inspired mineralization process. A range of natural gels based on agar,[4,5] gelatin[6,7], chitosan,[8] peptide,[9,10] β-CD,[11] and collagenous matrices[12] and other substrates[13] have been used as the gel substrate for the mineralization. For example, highly ordered biosilica with precise control over obtained inorganic material nanostructures was fabricated by the biomimetic synthesis using biomolecules and tetraethyl orthosilicate (TEOS) or tetramethyl orthosilicate (TMOS) as the templates and the precursor, respectively.[9] In addition, TiO_2 and other composite materials were synthesized by biomimetic mineralization using peptides as templates.[14] The CuS framework with porosity was fabricated *via* hydrothermal method using chitosan as a template, and the formation mechanism of the porous-structured CuS has been proposed. Furthermore, new templates for biomineralization include enzymes, egg white/eggshell, and protein. Using natural gels as substrates for mineralization, the composites have the advantages of excellent properties and good biocompatibility. However, the mineralization template is difficult to obtain and the production scale is small, which limits the application of the composites.

The synthetic polymer is highly flexible in terms of the available or accessible monomers, compositions, controllable size, molecular weights, and morphology. In the synthetic polymer, hydrogels are ideal models for researching the biomineralization or for the synthesis of new, advanced composites in biomaterials applications. The hydrogel is a cross-linked polymer with a network structure that is swollen in a suitable solvent.[15] They can be adjusted to special requirements by appropriate choice of monomers and crosslinkers. Compared with other synthetic polymers, hydrogels in the size, composition, and even crosslinking density are easily controlled by appropriately choosing the reaction condition, monomers, and crosslinkers. Their narrow size distribution combined with their advantages mentioned above makes them ideal templates for preparing spherical inorganic–organic composite materials.[16] For example, synthetic polymer hydrogels composed of poly(acrylamide),[17] PNIPAM,[18] polycaprolactone-*block*-poly(-acrylic acid),[19] and other materials have been used as the template for mineralization. Although there are a number of reports in the literature about the hydrogel with special patterned morphology, the pattern morphology of the composites formed on the surface of materials is derived from the oriented growth of crystals caused by additives or self-assembled templates. For instance, the results of the complex 3D dendritic nano architectures of copper hydroxide indicated that the morphology was caused by the effect of biological molecules on the branching growth of copper hydroxide crystals. To evaluate the relationship between the surface functionality and hierarchical morphology, Wang *et al.* synthesized a series of carboxylic-functionalized hydrogel/SiO_2 microspheres *via in situ* sol–gel reaction. The results showed that the surface carboxylic groups formed by hydrolysis of anhydride groups were the decisive factor to control the nucleation of nano-SiO_2 particles, and the PEG chains on the surface can affect the growth of the SiO_2 particles.[20] The research results show that the morphology of inorganic crystals is controlled by numerous parameters, such as pH, temperature, salt and polymer concentration, polymer molecular weight, polymer architecture or the presence of further compounds, in the gel media by primarily controlling the reactant ions' diffusion in their network structure, which affects nucleation and development at different points in time and space both naturally and technologically.

Recently, our group proposed a microgel template mineralization approach and developed innovated studies in the preparation of different composite microspheres by using the microgel template technique. Previous studies reported[21–27] the different pattern morphologies formed by the deposition of different metal sulfides or metallic oxide on the microgel template. It was found that the surface morphology is affected by varying the composition of the template,[21,22] the deposited inorganic ingredient,[23,24] structure of surfactants,[25] the kinds of inorganic-salts[22,26] and sulfide source.[27] The previous papers mainly focused on the interesting results of various patterned surface structures of metal sulfide deposition on the hydrogel surface,[21,22] whereas the formation mechanism is only a speculation, and these speculations are not reasonable to some extent. For example, as described in the literature,[21] the isopropyl groups of the copolymer, P(NIPAM-*co*-AA) near the interface might extend to the continuous phase due to their hydrophobic nature. The carboxyl groups of the co-polymer, however, might avoid contacting the organic phase, and extend inward. It is this self-separation that makes the structure of the interface of the microgels and the continuous phase uneven and heterogeneous. This complex interface structure might be the origin of the patterned surface structure of the composite microspheres. The above explanation is just speculation without relevant experimental evidence. In this report,[22] it has been revealed that the surface structures of these composite microspheres depend not only on the nature of the template, but also on the nature of the metal sulfide. It is speculated that the microgels mainly play roles of confinement and guidance in the precipitation of the sulfides. The explanation is general and short on detail. Therefore, it is necessary to study the mechanism on the formation of the zigzag patterned surface of the composite microspheres.

Based on a careful review of the published papers, this study aims to propose a new mechanism of the formation of the wrinkle pattern morphology by sulfide deposition on the hydrogel surface. In this study, various factors affecting the deposition of the metal sulfide on the hydrogel surface were taken as variables to obtain the corresponding composite microspheres. By observing the surface morphology characteristics of the corresponding composite microspheres, the corresponding factors affecting the wrinkle pattern morphology and its mechanism were determined. Based on the experimental results, the formation mechanism termed "the deformed shrinkage of the surface texture" was proposed. To understand the formation mechanism of the surface morphology in the composite microspheres, it is very important for mending the material defects, improving the material performance, and avoiding the materials decay in the process.

Open Access Article. Published on 24 November 2021. Downloaded on 2/10/2026 2:57:07 PM.
This article is licensed under a Creative Commons Attribution-NonCommercial 3.0 Unported Licence.

2. Experimental

2.1 Materials

N-Isopropylacrylamide (NIPAM) was purchased from ACROS. Acrylic acid (AA) was purified by distillation under reduced pressure prior to polymerization. The initiator (ammonium persulfate, APS), the cross-linker (*N*,*N*′-methylenebisacrylamide, BA), the promotor (*N*,*N*,*N*′,*N*′-tetramethylethylenediamine, TMEDA), Span-80, Tween-80, *n*-heptane, $Cu(Ac)_2$, H_3BO_3, HAc, ethylenediamine, NaCl, KCl and other chemicals were of analytical grade. The water used in this study was deionized and doubly-distilled.

2.2 Preparation of P(NIPAM-*co*-AA) microgels

Detailed information about the synthesis of P(NIPAM-*co*-AA) microgels has been reported in ref. 21. A 250 mL three-neck boiling flask was equipped with a mechanical stirrer, a nitrogen inlet and a Hirsch funnel. To the flask, 100 mL of *n*-heptane and 0.6 g of a neutral surfactant mixture formed by Span-80 and Tween-80 (5 : 1 in mass ratio) were added. The mixture was stirred vigorously under a N_2 atmosphere, until the surfactant was uniformly dispersed. At the same time, 1.2 g of NIPAM and AA (5%, weight percent), 0.06 g of BA and 1 mL of APS solution (216 mg mL^{-1} in aqueous phase) were dissolved into 6 mL double-distilled water. Then, the later solution was added into the flask *via* the funnel, and the new mixture was stirred continuously under a N_2 atmosphere. The reaction was initiated by addition of 1 mL of a promoter, TMEDA solution (50 mg mL^{-1}). The reaction was conducted under stirring (550 rpm) at 25 °C for 4 h. The P(NIPAM-*co*-AA) microgels were collected by filtration and washed alternatively with double-distilled water and acetone several times to remove the unreacted monomer and other impurities, and dried at room temperature.

2.3 Preparation of P(NIPAM-*co*-AA)/CuS composite microspheres

Preparation of the CuS-containing composite microgels has been performed by the method described in our previous research.[24] The composite microspheres were prepared *via* two steps. In a typical synthesis, 0.3 g of P(NIPAM-*co*-AA) microgels with 20% (weight percent) of AA was swollen in 1.2 mL of $Cu(Ac)_2$ solution (0.1 mol L^{-1} in water). Then, the microgels containing Cu^{2+} were suspended in 75 mL of *n*-heptane with mild stirring. The suspension was stirred for 40 min after addition of the metal-containing microgels, and H_2S was then introduced slowly for 30 min under constant stirring. The suspension was further stirred for another 3 h before separation by centrifugation. The dark brown composites of P(NIPAM-*co*-AA)/CuS were collected and washed alternatively with double-distilled water and acetone for several times and dried in air. The preparation process of P(NIPAM-*co*-AA)/CuS is shown in Scheme 1.

Some conditions for the preparation of the P(NIPAM-*co*-AA)/CuS composite microspheres with different conditions are shown in Table 1.

Other composite microspheres with the addition of other reagents were prepared in a similar way. It is important to note that the needed additives are narrated in the experiments in detail.

2.4 Characterization

The morphologies of the P(NIPAM-*co*-AA) microgels and the P(AM-*co*-MAA)/CuS composite microspheres have been examined by Philips scanning electron microscopy (SEM, XL-20). The preparation process of the samples before measurement is as follows: 5 mg of the samples were dried in an oven for 4 h, and evenly spread out on the sample stage, then coated with a thin layer of gold. Finally, these samples were tested in SEM equipment with an accelerating voltage of 20 kV. The IR spectra were recorded on an AVTAR360 Nicolet FTIR spectrometer using KBr pellet. The sample was spread uniformly and in a single layer on the sample table.

3. Results and discussion

3.1 Morphology of P(NIPAM-*co*-AA) microgels

The polymer gel is a three-dimensional network filled with solvent. In many cases, the hydrogel undergoes extensive

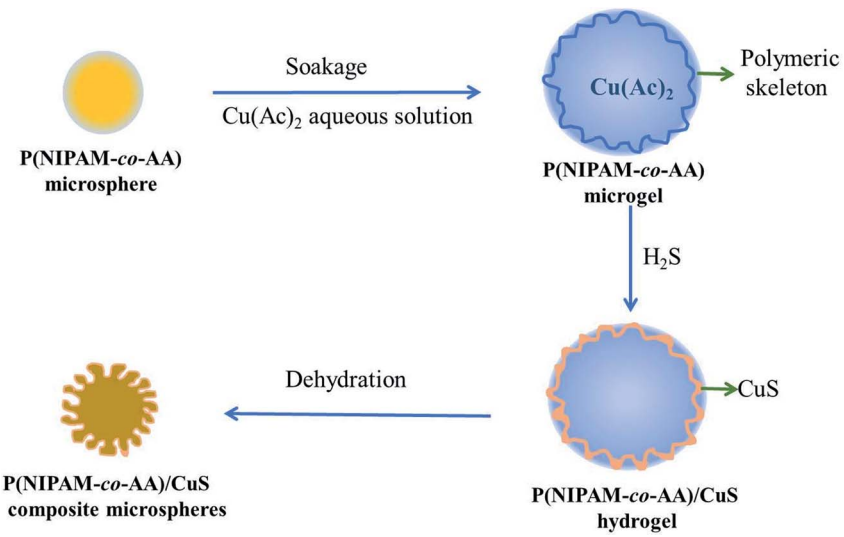

Scheme 1 The preparation process of P(NIPAM-*co*-AA)/CuS.

© 2021 The Author(s). Published by the Royal Society of Chemistry

Open Access Article. Published on 24 November 2021. Downloaded on 2/10/2026 2:57:07 PM.
This article is licensed under a Creative Commons Attribution-NonCommercial 3.0 Unported Licence.

Table 1 Some conditions for the P(NIPAM-*co*-AA)/CuS composite microspheres[a]

P(NIPAM-*co*-AA)/CuS sample	Swelling degree[b]	Acidity[c]	Ionic strength[c]	Amount of surfactant[c] (g)	Introducing speed of H_2S[c] (mL s^{-1})	Stirring rate[c] (rpm)
Fig. 3	Freeze-drying, place in a H_2O atmosphere or dense H_2SO_4 atmosphere with different time					
Fig. 4		HAc, H_3BO_3, ethylenediamine, pH = 5.6, 9.2				
Fig. 5			NaCl, KCl			
Fig. 6				0.07, 0.17, 0.37		
Fig. 7					0.04, 0.25, 1.5	
Fig. 8						300, 500, 1000

[a] All factors selected in the column head row of the table stem from the following considerations. Different swelling degree, acidity degrees, ionic strength, amount of surfactant, introducing speed of H_2S and stirring rate of the P(NIPAM-*co*-AA)/CuS composite microspheres for exploring the formation mechanism of the P(NIPAM-*co*-AA)/CuS composite microspheres. [b] The microgel swollen $Cu(Ac)_2$ solutions were treated first by freeze-drying, and then deposited after placing in a H_2O atmosphere for 1 day, 5 days. Comparing the above study, the microgels swollen $Cu(Ac)_2$ solutions were deposited after placement in a dense H_2SO_4 atmosphere for 12 h and 18 h. The other conditions for the preparation of the P(NIPAM-*co*-AA)/CuS composite microspheres are the same as those in Section 2.3 in the text. [c] The other conditions for the preparation of the P(NIPAM-*co*-AA)/CuS composite microspheres are the same as those in Section 2.3 in the text.

volume change in response to external stimuli. Various kinds of patterns have also been observed if the volume changes fast enough in either swelling or shrinking.[28] The pattern formation has been intensively studied since it is believed to be helpful to elucidate the mechanical properties of the gels and pattern evolutions in biological systems.[29] The swelling patterns of hydrogels have been reported in the literature, where the polymeric gels are usually spherical, slab-like, and cylindrical.[30,31] A typical swelling process has been reported by Tanaka *et al.*,[28] when a spherical hydrogel with smooth surface swelled, regular patterns was observed on the surface, then coalesced and eventually disappeared. Permanent patterns are also observed on the mechanically constrained gel slab. Additionally, the unswollen core constrains the swelling region, and thus leads to pattern formation in the wetted region. Although the composition of our composite microspheres with pattern is different from the hydrogel mentioned above, based on the results we reported,[21–27,32,33] the patterned structures of the composite microspheres made by *in situ* deposition of inorganic ingredients on the microgel were seemingly related to network distortion of the microgel surface instead of the crystal appearance of the inorganic components. So, in this paper, the formation mechanism on the patterned surface of the P(NIPAM-*co*-AA)/CuS composite microspheres was mainly concentrated to research on factors related to the deformation of the P(NIPAM-*co*-AA) gel networks as CuS *in situ* formed.

The patterned structures of the composite microspheres made by *in situ* deposition of inorganic ingredients on the microgels were seemingly related to the network distortion of the microgel surface. So, it is necessary to characterize the framework structure of the P(NIPAM-*co*-AA) microgel. The samples used for SEM measurements were quickly frozen in liquid nitrogen and freeze-dried for 1 day. The typical SEM images are shown of the water-swollen (Fig. 1a) and $Cu(Ac)_2$ solution-swollen (Fig. 1c) P(NIPAM-*co*-AA) microgels after freeze-drying. It can be clearly observed that the microgels are near spherical with a porous structure. These results imply that there are polymer framework structures and a water domain in the swelled microgels before the deposition. The SEM image for a hydrogel quickly frozen in liquid nitrogen followed by freeze-drying has been observed.[34] The micrographs of hydrogels for PNIPAM also indicated a sponge-like microporous structure. The causes for the formation of this porous feature have been studied. Matsuo *et al.*[35] have presented a general picture for the physical principle underlying the formation of spatial inhomogeneities in polymer gels. They concluded that there were three types of causes for the structural inhomogeneities within

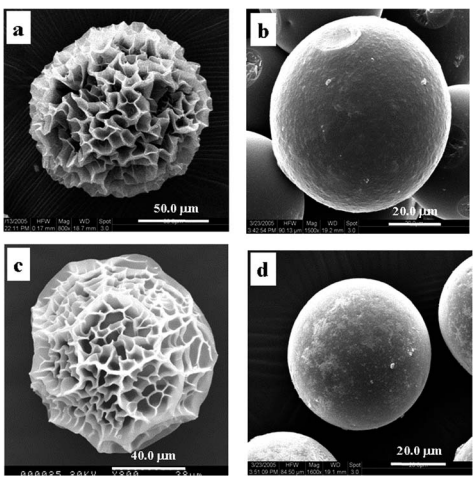

Fig. 1 SEM images of the swollen microgels in different dehydration methods. Water-swollen microgels after freeze-drying (a) and washing with acetone (b); $Cu(Ac)_2$ solution-swollen microgels after freeze-drying (c) and washing with acetone (d).

Open Access Article. Published on 24 November 2021. Downloaded on 2/10/2026 2:57:07 PM.
This article is licensed under a Creative Commons Attribution-NonCommercial 3.0 Unported Licence.

a gel. First, the dynamic concentration fluctuations of pregel polymer solutions are frozen in the final network structure upon the onset of the gelation process. Second, if the polymer solution is in the phase separation regime, there appear two gel phases having two different concentrations. In both cases, the phase equilibrium properties of the gel play an essential role in determining the permanent structural inhomogeneities within a gel. Third, in addition to having these permanent structural inhomogeneities, a gel undergoes temporal thermal concentration fluctuations. The permanent inhomogeneities contribute to the phenomenon of the nonergodicity of a gel. Therefore, the sponge-like microporous structure of the water swollen P(NIPAM-*co*-AA) microgel after freeze-drying can be understood. As for the $Cu(Ac)_2$ solution-swollen P(NIPAM-*co*-AA) microsphere with porous structure, it is attributed to the Cu^{2+} coordination with acryl or carboxyl groups of the polymer or physical absorption by the polymer making $Cu(Ac)_2$ dispersion in frameworks. According to the research studies on the coordination between the metal ion and PNIPAM or PAA,[36,37] the coordination between Cu^{2+} and P(NIPAM-*co*-AA) is possible. From the SEM images, although there is the coordination between the metal ion and polymer, this interaction is limited to affect the framework structure of the microgel.

According to the protocol for the preparation of the composite microspheres of P(NIPAM-*co*-AA)/CuS, the composite microspheres were washed with acetone. It is worth obtaining the information about the effect of acetone on the morphology of the microgels. Interestingly, it can be seen in Fig. 1 that the surface of the water-swollen P(NIPAM-*co*-AA) microspheres (*cf.* Fig. 1b) or the surface of $Cu(Ac)_2$ aqueous solution (*cf.* Fig. 1d) treated with acetone becomes smooth, which demonstrates that acetone strongly affects the surface morphology of the microgel. It has been found that the polymer network of a gel, under certain conditions, undergoes a discrete transition in equilibrium volume with changes in the solvent composition. Ionization of the gel network plays an important role in the phase transition. A nonionized acrylamide gel immersed in acetone–water mixtures shows a continuous change in the equilibrium volume when the acetone concentration is changed. If a small portion of the acrylamide groups in the network is hydrolyzed into ionizable acrylic acid groups, a reversible volume collapse as large as 350-fold occurs when the acetone concentration is increased.[38] The mechanical and swelling behavior of the ionized networks of copolymers of acrylamide with sodium methacrylate in acetone–water mixtures have been studied.[39] The results illustrate that the volume network and modulus value in the phase transition exhibit jump-wise changes, and the change in modulus adequately correlates to a volume change in the network collapse. Based on our experiments and the literature mentioned above, the fact that the surfaces of water-swollen or $Cu(Ac)_2$ solution-swollen P(NIPAM-*co*-AA) microgels are smooth after the microgels are washed by acetone are related to the swollen microgel network collapse made by acetone. The water-swollen or $Cu(Ac)_2$ solution-swollen P(NIPAM-*co*-AA) microgels after freeze-dried treatment are of the porous structure, indicating that water in the P(NIPAM-*co*-AA) microspheres swollen by $Cu(Ac)_2$ solution is located in the porous part of the swollen microgels before *in situ* preparation of the P(NIPAM-*co*-AA)/CuS composite microspheres. Compared to the surface morphology of the naturally dried and freeze-dried hydrogels in Fig. 1, it indicates that the polymeric skeleton with irregular pore structure did exist on the surface of the undeposited hydrogel when the metal sulfides were deposited *in situ* on the hydrogels. It is speculated that Cu^{2+} complexed with the side chain groups of the polymeric skeleton in the hydrogel surface, and the Cu^{2+} reacted with H_2S encountered at the interface to form more stable CuS precipitation, which was deposited on the polymeric skeleton on the hydrogel surface. Thus, the rigidity of the polymeric skeleton in the deposition region is enhanced.

In order to verify the effect of acetone on the surface pattern of the composite microspheres, the freeze-dried P(NIPAM-*co*-AA)/CuS microspheres saturated with water were prepared. Representative SEM micrographs are given in Fig. 2. It can be seen that the surface morphologies present a regular evolution with dehydration, as expected. Fig. 2a and d shows the water-saturated P(NIPAM-*co*-AA)/CuS composite microspheres after freeze-drying, indicating that the composite microspheres remain basically similar to the freeze-drying sample of the hydrogel (Fig. 1a and c) when the hydrogel in the composite microspheres does not shrink. Acetone has the property of dehydrating hydrogels, and the higher the concentration of acetone in aqueous solution, the greater the degree of hydrogel contraction. It is believed that the morphology of the composite microspheres is related to water loss of the composite microspheres. Therefore, the composite microspheres were prepared by impregnating the composite microspheres with aqueous acetone and pure acetone, respectively, then treated by freeze-drying. As shown in Fig. 2b, e and c, f, the larger the shrinkage of the composite microspheres, the denser the surface wrinkle of the composite microspheres. The results are consistent with the expected results. Obviously, the surface wrinkle morphology is related to the shrinkage of composite microspheres. The contractibility originates in the dehydration of the microgel, and the heterogeneity derives from the heterogeneous distribution of the CuS deposited on the surface of the microgel, which result in the rigidized difference of the polymeric frameworks on the microgel surface.

The smooth morphology of the composite microspheres appears when the matrix has the same properties. However, the existence of an internal network structure makes the scalability of the matrix uneven when a matrix with a different property is used. This is the essential reason for the appearance of the surface morphology.

3.2 Morphology of the P(NIPAM-*co*-AA)/CuS composite microspheres

From the conclusion mentioned above, all factors related to the contractibility of the microgel and distribution of the CuS deposited on the surface of microgels should be considered to explore the causes for the P(NIPAM-*co*-AA)/CuS microspheres with varied surface zigzag patterns. Although the factors are diversified, the main factors resulting in the surface zigzag

© 2021 The Author(s). Published by the Royal Society of Chemistry

Open Access Article. Published on 24 November 2021. Downloaded on 2/10/2026 2:57:07 PM.
This article is licensed under a Creative Commons Attribution-NonCommercial 3.0 Unported Licence.

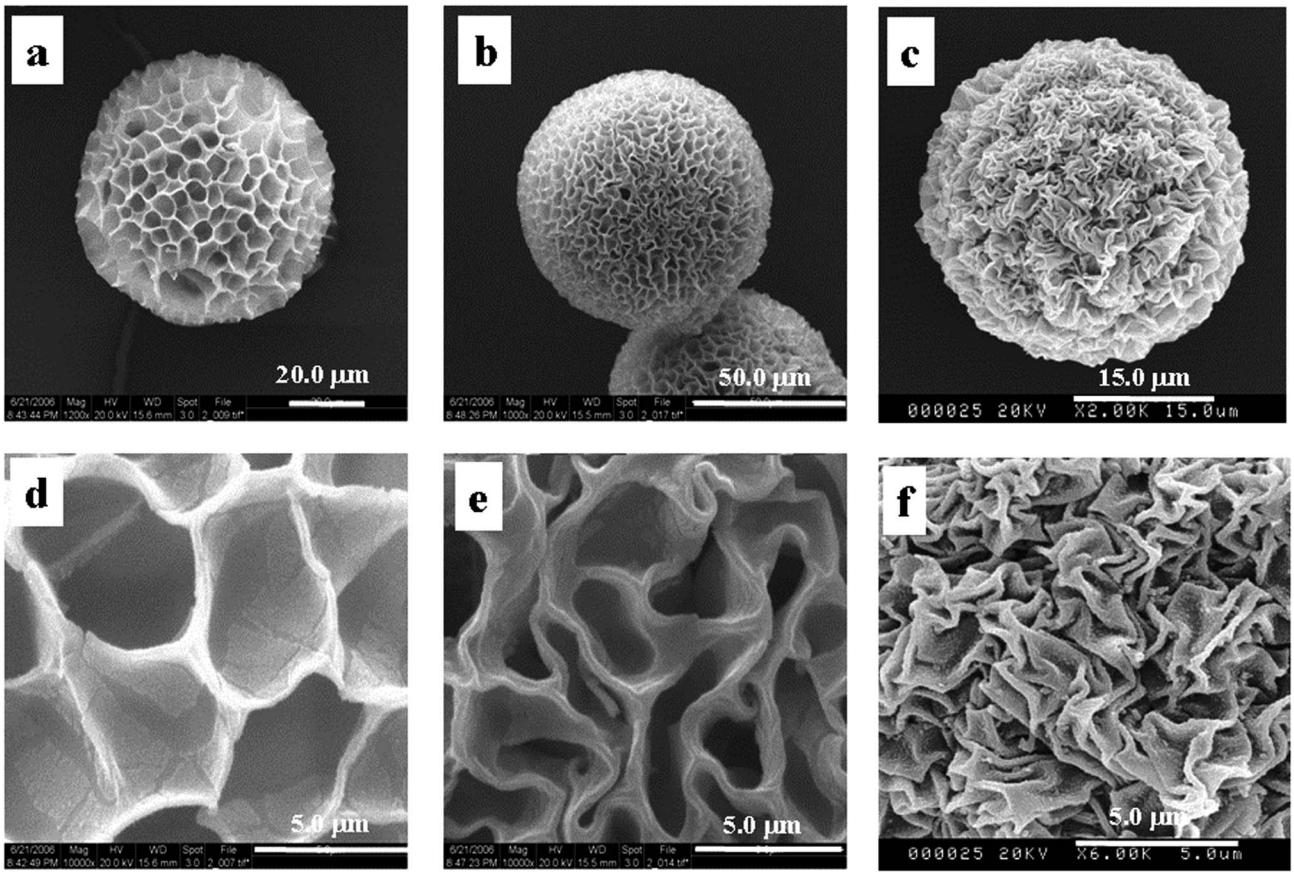

Fig. 2 SEM images of water-saturated P(NIPAM-*co*-AA)/CuS composite microspheres after freeze-drying (a and d). The partially dehydrated composite microspheres with a mixture of aqueous acetone are then treated by freeze-drying (b and e), and the completely dehydrated composite microspheres with acetone (c and f).

patterns are expected to be brought to light. Here are some results as follows. If the framework of the microgels having softness is the imminent factor for the changeability of the template framework then there is relevance between the applied factors and surface structures of composite microspheres. At one time, if deposits do not result in the deformability of framework by themselves, the changing factors must be from the precipitation reaction. There are numerous effect factors in the deposit reaction, such as the introduction speed of hydrogen sulfide, the stirring rate, the dosage of surfactant, and the adding salt.

3.2.1 Effect of swelling degree of microgels. In order to further explain that the shrinkage degree of hydrogel microspheres is related to the surface wrinkle morphology of the composite microspheres, P(NIPAM-*co*-AA)/CuS was prepared by depositing on hydrogel surfaces of different swelling degrees. Fig. 3 depicts the SEM images of P(NIPAM-*co*-AA)/CuS microspheres prepared in different swelling degrees of the microgels. The freeze-drying composite microspheres with different swelling degrees were obtained by placing deposited copper sulfide composite microspheres in water for different swelling times. The composite microspheres with different swelling degrees were dehydrated in a concentrated H_2SO_4 dryer for different times to obtain the composite microspheres with different shrinkage degrees. The Cu(Ac) solution-swollen microgels were first treated by freeze-drying, and then placed in the gas phase of a closed container in the presence of water for a given time in order to get different swelling degree microgels. After that, the composite microgels were prepared according to the procedure stated in Section 2.3. It can be found that the surface wrinkles of the microspheres became gentle with treated time. The microgels placed in the gas phase with a longer time result in increasing the swelling degree due to the increase of water absorbed by the microgels. As the preceding conclusion, the surface heteromorphosis of the composite microspheres depends on the heterogeneous contractibility of the polymeric frameworks in the microgel. So, it is not difficult to understand that the swelling degree of the microgels before deposition affects the morphology of the composite microspheres. The results show that the surface wrinkle pattern morphology is related to the shrinkage degree of the composite microspheres.

In order to prove the effect of the pore size of the template on the zigzag patterned structure, the following experiments are particularly designed, in which the template is swelled in a mixed solution of acetone and water of different ratios due to the dissimilar swelling degree of the template (the template is swelled in water for the polymer has water-solubility, while it is contracted in acetone). Fig. 3 depicts the SEM images of the template by swelling in acetone and water of different ratios

Open Access Article. Published on 24 November 2021. Downloaded on 2/10/2026 2:57:07 PM.
This article is licensed under a Creative Commons Attribution-NonCommercial 3.0 Unported Licence.

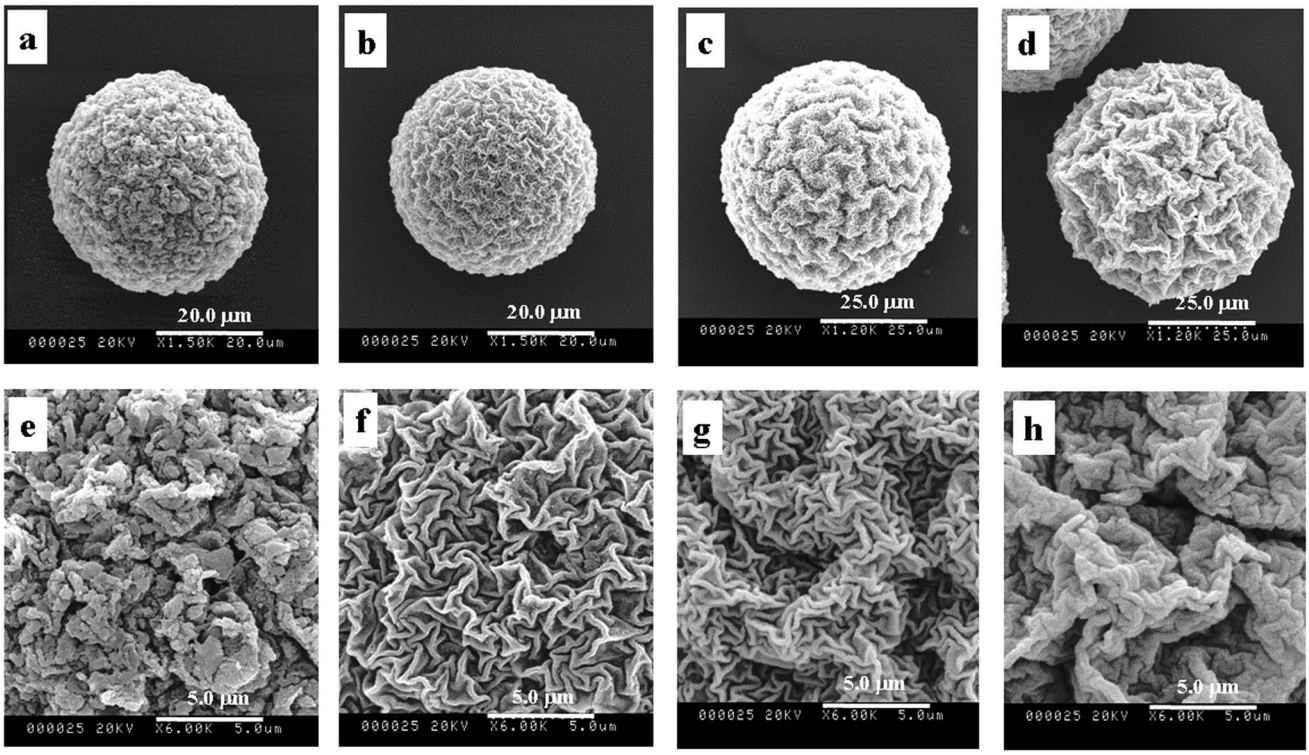

Fig. 3 SEM images of P(NIPAM-*co*-AA)/CuS microspheres prepared in different swelling degrees of P(NIPAM-*co*-AA) microgels. The microgels swollen $Cu(Ac)_2$ solutions were treated first by freeze-drying, and then deposited after placement in a H_2O atmosphere for 1 day (a and e), 5 days (b and f). Comparing the above study, the microgels swollen $Cu(Ac)_2$ solutions were deposited after placement in a dense H_2SO_4 atmosphere for 12 h (c and g), and 18 h (d and h).

after freeze-drying. For example, the microgels are dealt with water (Fig. 3a and e), 3 : 1 (in volume ratio) of acetone and water (Fig. 3c and g) and 10 : 1 (Fig. 3d and h), respectively. Compared with the surface of the microspheres in Fig. 3, it can be seen that the more water is used, the bigger size of pore and the wider edge appear (Fig. 3a and e) or *vice versa* (Fig. 3c and g). When microgels are swelled in the acetone solution of higher content, there is hardly a pore structure (Fig. 3d and h), indicating that the polymeric framework deforms due to dehydration, that the dehydration effects actually destroy the interaction force between the water molecule and polymeric chain, and that the action of the hydrogen bond of the intra-polymeric chain increases. So, there is the relevance between the deformation extent and degree of dehydration. We can conclude that the frameworks and the rich-water domains exist in the swelled microspheres, and this shows the relevance between the surface structure of the complex microspheres and the zigzag patterned structure to some extent.

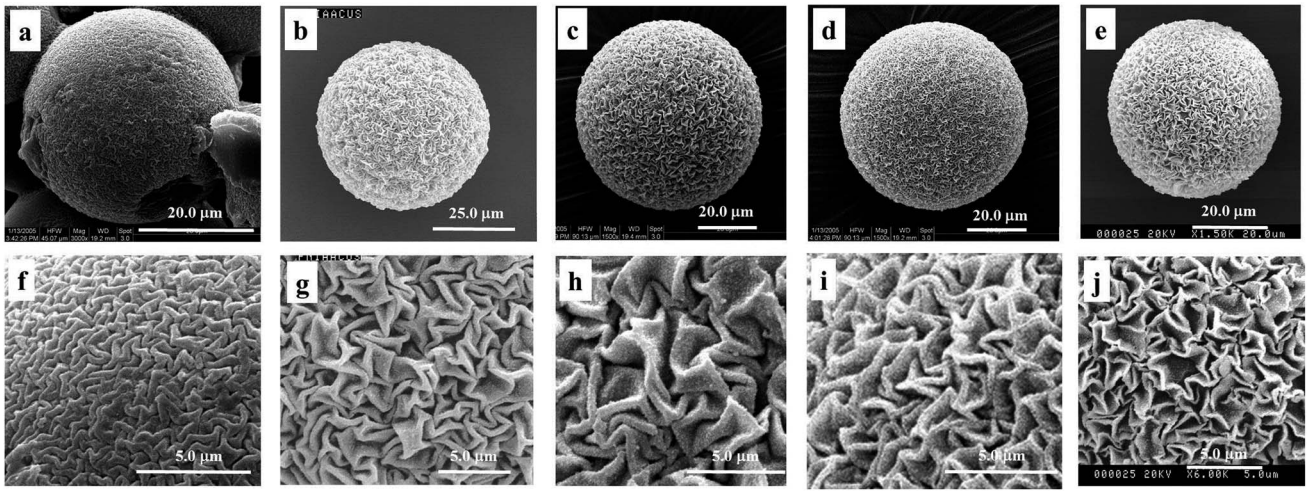

Fig. 4 SEM images of P(NIPAM-*co*-AA)/CuS adding HAc (pH = 3) (a and f), H_3BO_3 (b and g), ethylenediamine (c and h), pH = 5.6 (d and i) and pH = 9.2 buffer solution (e and j).

© 2021 The Author(s). Published by the Royal Society of Chemistry

Open Access Article. Published on 24 November 2021. Downloaded on 2/10/2026 2:57:07 PM.
This article is licensed under a Creative Commons Attribution-NonCommercial 3.0 Unported Licence.

3.2.2 Effect of acidity and ionic strength in the $Cu(Ac)_2$ solution. Fig. 4 is a series of SEM images of the composite microspheres of precipitation CuS after swelling by using $Cu(Ac)_2$–HAc solution (see Fig. 4a and f), and $Cu(Ac)_2$–H_3BO_3 solution (see Fig. 4b and g), $Cu(Ac)_2$–ethylenediamine solution (see Fig. 4c and h), and pH = 5.6 (d and i) and pH = 9.2 buffer solution (e and j). It can be seen that compared with the composite microspheres treated with $Cu(Ac)_2$–H_3BO_3 solution or $Cu(Ac)_2$–ethylenediamine solution, the surface morphologies in the $Cu(Ac)_2$–HAc solution are finer. The difference of the surface structure may be explained by the following process: inorganic ions absorbed in the swelled microgels reacted ceaselessly with introducing hydrogen sulfide (H_2S) gas on the interface between oil and water, and then diffused into the interior in direct precipitation. There are two reasons for the phenomenon. To begin with, precipitation took place on the framework of microspheres having more metal ion due to interaction between the metal ion and polymeric framework. The rigidity of the framework becomes strong as the reaction of the deposition happens on the framework, while the other domain changes and becomes softer. At one time, the distortion of framework comes from the precipitation reaction making poor hydrophilicity, and dehydration appears to some extent. In addition, protons were continuously released with the precipitation reaction and microspheres were contracted definitely by the action. However, microspheres have contracted on the whole before precipitation due to the template having pH-stimuli, such that the pH-dependent swelling behavior of the polymer microgels mattered in different acidities. So, the relative dense wrinkles of the surface morphologies were formed (see Fig. 4a and f) due to the decrease of the shrinkage degree again in the strong acidity of HAc. Nevertheless, the surface morphology of the composite microspheres in the $Cu(Ac)_2$–ethylenediamine solution is similar to those in the $Cu(Ac)_2$–H_3BO_3 solution. The shrinkage in the $Cu(Ac)_2$–ethylenediamine solution on the whole is weaker than that in the $Cu(Ac)_2$–H_3BO_3 solution, and the shrinkage degree of the microspheres decreases again due to the weak acidity of H_3BO_3, and the wrinkles become deeper (see Fig. 4b and g). However, on adding to ethylenediamine, the swelling degree of the microspheres increases greatly and the shrinkage of the microspheres becomes greater and finally deeper wrinkles form. Furthermore, S^{2-} prefers to release in an alkaline environment; the lower the pH value is, the lower the release rate becomes. As a result, the effects of ethylenediamine on the surface morphology of the composite microspheres are similar to that of H_3BO_3.

In addition, the microsphere morphologies after freeze-drying under the different acidity conditions were examined to prove the relevance between the effect of the surface morphology and the swelling degree. These results suggest that the pore of the microgels was contracted under the acidity conditions. Additionally, the volume collapse can be induced by varying the pH of the gel fluid.[39] Analyzing the above results, we can draw a conclusion that the zigzag patterned surface was affected by the acidity of the medium in precipitation. If the effects were eliminated by buffer solution, we can obtain composite microspheres having the similar patterned surface. Therefore, the experiments being treated with buffer solution of the different acidity were designed. As can be seen in Fig. 5, the surface

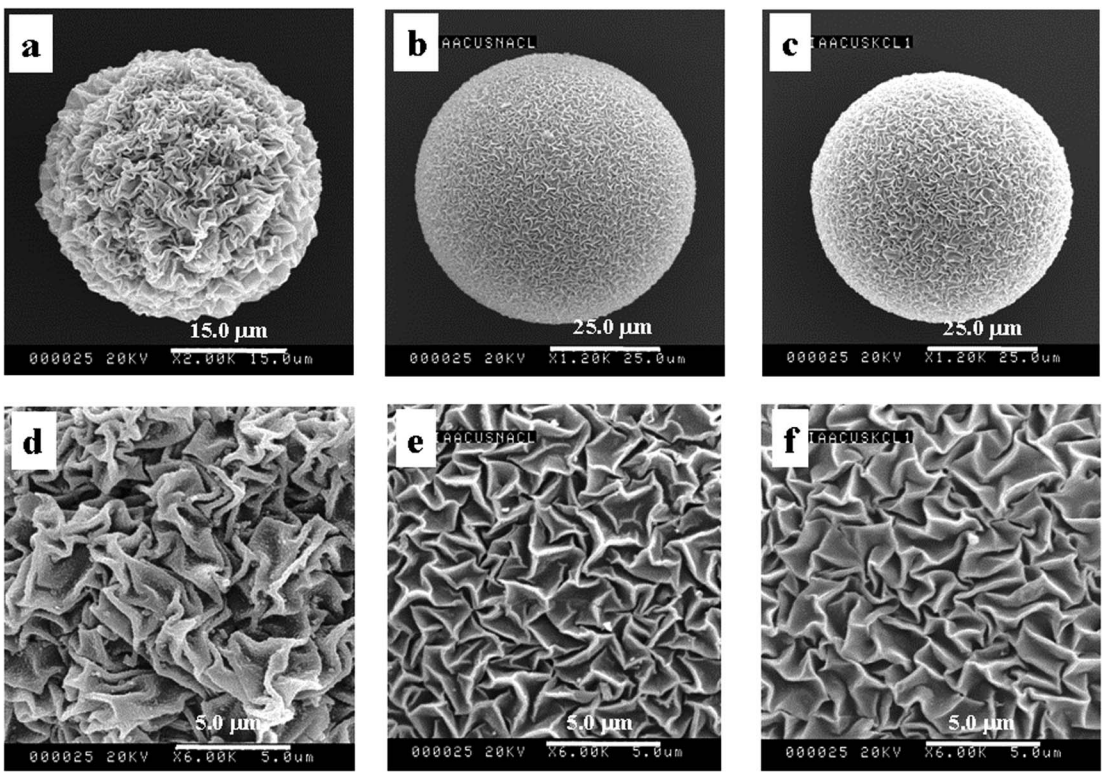

Fig. 5 SEM images of P(NIPAM-*co*-AA)/CuS of no additive (a and d) and adding NaCl (b and e) and KCl (c and f).

© 2021 The Author(s). Published by the Royal Society of Chemistry

Open Access Article. Published on 24 November 2021. Downloaded on 2/10/2026 2:57:07 PM.
This article is licensed under a Creative Commons Attribution-NonCommercial 3.0 Unported Licence.

morphologies conform to our conceivable plan, in which surface morphologies become comparatively fine (Fig. 4d and e) as the effects releasing the proton during precipitation were eliminated because of the influence of the buffer solution. However, the wrinkle structure in basic buffer solution (Fig. 4d and i) is greater than that in acidic buffer solution (Fig. 4e and j) since the microspheres have strong contracting under conditions of strong swelling of microspheres in alkaline solution. Contrasted with the 'adding buffer solution' condition, the composite microspheres under the 'adding no buffer solution' conditions show a deep structure. The acidity increases with releasing protons in precipitation, which results in composite microspheres contracting on the whole, and produces additional wrinkles of second shrinkage. So, it can be concluded that the zigzag patterned surface morphology is affected by releasing protons during the deposit reaction.

Fig. 5 shows the SEM images of different additives. No additive is in Fig. 5a and d, and adding NaCl and KCl are in Fig. 5b, e and c, f, separately. It is clearly demonstrated that the surface morphologies were affected by the additive, and the surface structure after adding salt becomes very fine. There are two main reasons as follows. First, the hydrated action makes the molecules of the solution bonded water-layer move with difficulty. Second, the ionic migration was hampered by the inverse ion when the positive and negative ions were in inverse ionic atmosphere, according to the model of Debye–Huckel ion atmospheres. Furthermore, the effect of adding NaCl is similar to KCl on the surface morphologies of the composite microspheres, which is relevant to the property of salt. The two factors result in difficult dehydration and the migration of protons was inhibited. Thereby, the surface morphologies of adding salt are shallower than that of no additive.

The charged hydrogel swelling was investigated as a function of solution ionic strength by John M. Prausnitz *et al.*[40] The results indicated that the ionic strength is an essential factor to affect the swelling of the hydrogels. The swelling capacity of the hydrogels obviously decreased with increasing ionic strength because the repulsions between the fixed charged groups and the gel were shielded and the deswelling of gel is also happened.

An ionized acrylamide gel was found to undergo a discrete phase transition in equilibrium volume upon varying the salt concentration in the solution. The salt concentration required for the transition depends strongly on the valence of the positive salt ion added to the solution. In certain cases, the concentration at the transition is many thousand times larger for monovalent ions than for divalent ions. A simple theoretical consideration of the osmotic pressure of the ions can explain the phenomenon.[41]

As far as the template is concerned, the swelling behavior of microgels directly affects the deformability of the polymeric framework from the above experimental results. As a result, the model of the framework structure of the microsphere is put forward in different swelling degrees (Fig. 6). It can be seen that the stretching behavior of the microspheres exhibits being affected by solution, and the polymeric framework was contracted in acetone, but was completely stretched in water.

In summary, the swelling microgels are shown in the 3D network structure. The polymeric framework is soft to some extent and its framework definitely deforms. The surface morphologies form because the framework structures undergo deformation in the deposit reaction of CuS at the different swelling degrees. Meanwhile, no prominent characteristic peak from the results of XRD of the composite microspheres shows

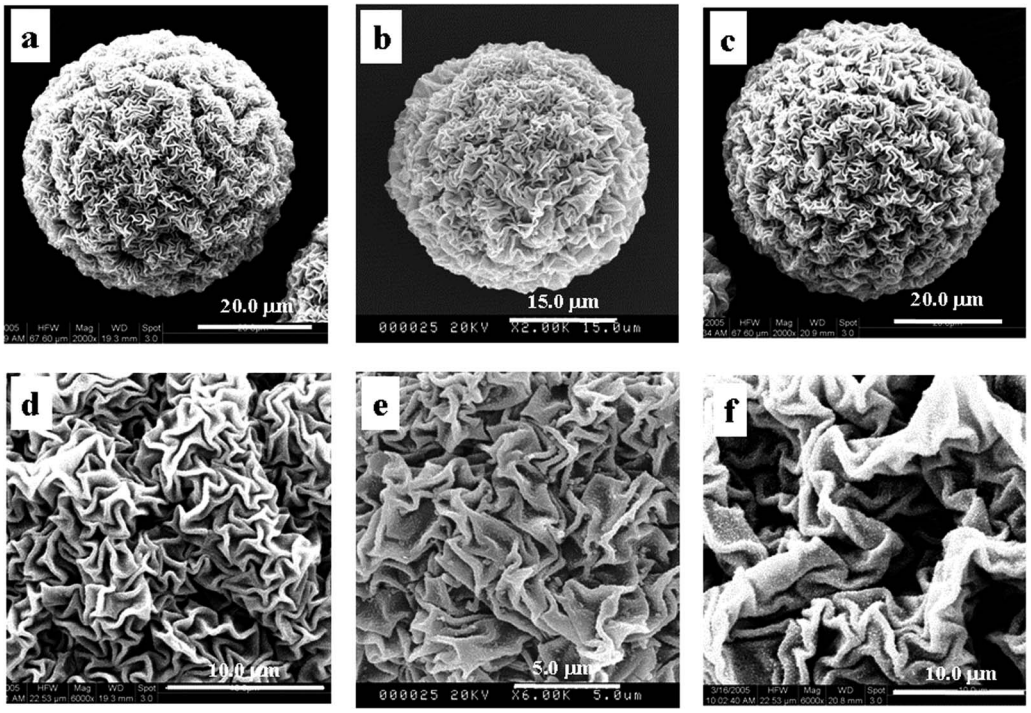

Fig. 6 SEM images of P(NIPAM-*co*-AA)/CuS in different surfactants (0.07 g (a and d), 0.17 g (b and e) and 0.37 g (c and f)).

© 2021 The Author(s). Published by the Royal Society of Chemistry

Open Access Article. Published on 24 November 2021. Downloaded on 2/10/2026 2:57:07 PM.
This article is licensed under a Creative Commons Attribution-NonCommercial 3.0 Unported Licence.

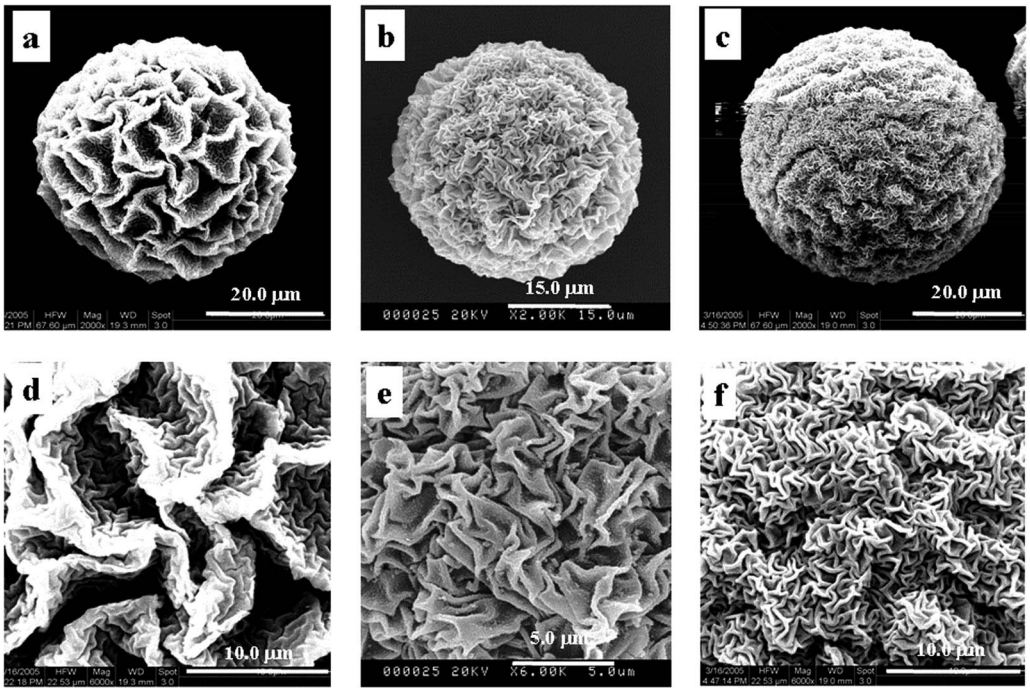

Fig. 7 SEM images of P(NIPAM-*co*-AA)/CuS in different introducing rates of H_2S (0.04 mL s^{-1} (a and d), 0.25 mL s^{-1} (b and e) and 1.5 mL s^{-1} (c and f)).

that the size of the deposit is small, and the scale of wrinkles of surface morphology is greater than the size of the deposit.[21] The results support the conclusion that the surface morphology is deformability of the framework structure. Namely, the surface morphology mainly originates from the contractibility of the composite microspheres.

3.2.3 Effect of the amount of surfactant. Fig. 6 is a series of SEM images of adding surfactant for 0.07 g (see Fig. 6a and d), 0.17 g (see Fig. 6b and e), and 0.37 g (see Fig. 6c and f), respectively. It is observed that with increasing dosage of surfactant added to the reaction system, the deeper the wrinkles of the surface morphologies become. It is known that there

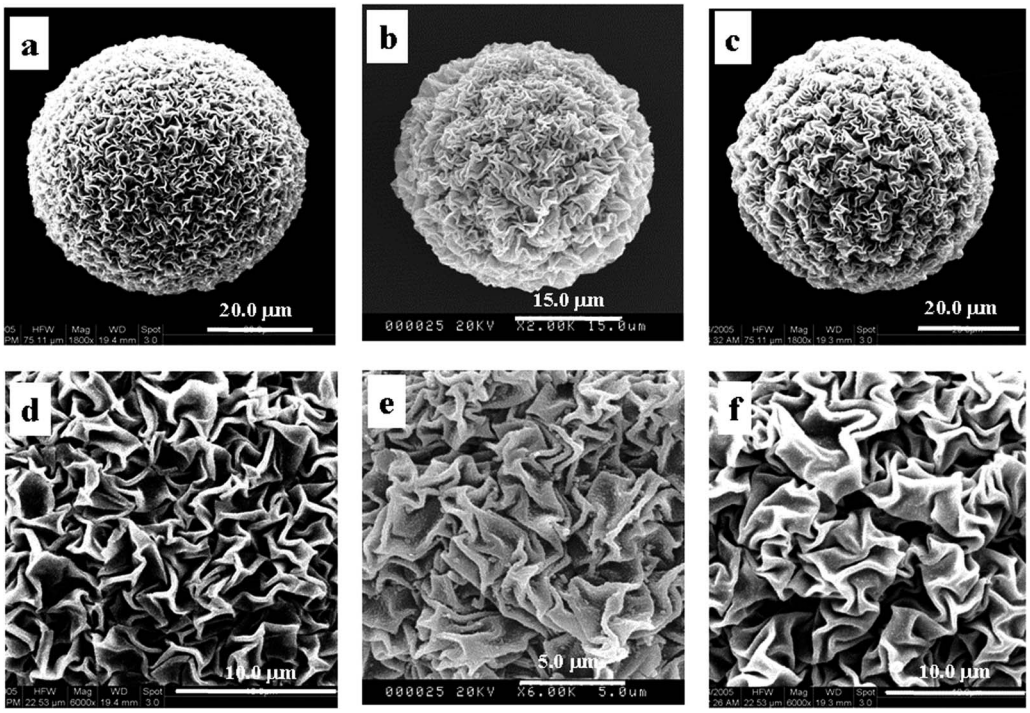

Fig. 8 SEM images of P(NIPAM-*co*-AA)/CuS in different stirring rates (300 rpm (a and d), 500 rpm (b and e) and 1000 rpm (c and f)).

© 2021 The Author(s). Published by the Royal Society of Chemistry

Open Access Article. Published on 24 November 2021. Downloaded on 2/10/2026 2:57:07 PM.
This article is licensed under a Creative Commons Attribution-NonCommercial 3.0 Unported Licence.

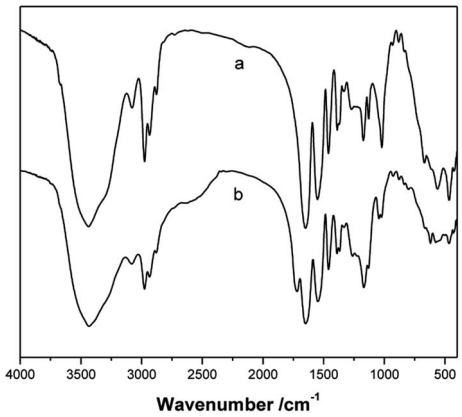

Fig. 9 FTIR spectra of the PNIPAM (a) and P(NIPAM-*co*-AA) (b) microgels.

exists a solution interface between heptane and the swelled microgel, and the addition of surfactant (Span 80) is very likely to modify the interfacial intension, and constantly affects the diffusion and growth of the nuclei of CuS.[42] The greater the dosage of surfactant added, the more absorbed water leaves and enters the oil phase, and the more contraction of the surface structures occurs. It is in accordance with the effect of the stirring rate on surface morphology.

3.2.4 Effect of the introducing speed of H_2S. Fig. 7 shows the SEM images of the different introducing rates of H_2S. It is easily observed that the surface morphologies become smooth with the introducing rate of H_2S. Combined with the above relevant results, the study shows the CuS prepared decreases with the decrease of the introducing rate of H_2S, in which the surface softness of the composite microspheres becomes strong and the shrinkage is very easy. Simultaneously, hydrogen ions produced in deposit reaction have enough time to diffuse into the microsphere interior. This is because the whole microspheres were affected by the diffused proton of the interior, and result in occurring second-shrinkage (see Fig. 7d). However, the formed rigid surface of the composite microspheres leads to forming an uneasy contracting domain when the introducing rate of H_2S is enhanced. The H^+ diffusion rate becomes slow and the whole microgels cannot easily undergo shrinkage, which shows the clear zigzag patterned surface (see Fig. 7d and f).

In a word, when CuS forms, the different introducing rates of H_2S have the different abilities of releasing protons and affecting the special zigzag patterned surface structures to a great extent.

3.2.5 Effect of the stirring rate in the precipitation reaction. Fig. 8 depicts the SEM images of different stirring rates, which is 300 rpm (see Fig. 8a and d), 500 rpm (see Fig. 8b and e), 1000 rpm (see Fig. 8c and f), respectively. From Fig. 8, it can be seen that the wrinkles of the surface become gradually clear with the increase of the stirring rate. It is well known that the formation of CuS is quite rapid and varieties of exoteric factors (such as stirring rate) are incapable to influence the rate of the precipitation reaction. Hereby, the lower the stirring rate is, the lesser the water loss, and the smoother the surface is (Fig. 8a and d) or *vice versa* (Fig. 8e and f).

To sum up, the ability of holding water becomes weak as the stirring rate increases, and the dehydration degree in which the absorbed water was extruded from the template into the oil phase becomes strong, which results in the shrinkage of the template and the special surface structure with the quick stirring rate.

3.3 Analysis of the components and characterization of the composite microspheres

FTIR analysis of the P(NIPAM-*co*-AA) microgels and PNIPAM microgels confirmed the presence of AA in the P(NIPAM-*co*-AA) microgels. The FT-IR spectra of the P(NIPAM-*co*-AA) microgels and the PNIPAM microgels are displayed in Fig. 9, respectively. Compared with PNIPAM microgels, besides the deformation of the two methyl groups on $-C(CH_3)_2$ at 1366 cm^{-1} and 1387 cm^{-1}, $-CH_3$ and $-CH_2-$ deformation at 1460 cm^{-1}, secondary amide N–H stretching, amide II band at 1551 cm^{-1} and amide I band at 1648 cm^{-1}, $-CH_3$ symmetric stretching at 2877 cm^{-1}, asymmetric $-CH_2-$ stretching at 2934 cm^{-1}, $-CH_3$ asymmetric stretching at 2975 cm^{-1}, N–H stretching at 3437 cm^{-1},[43] the characteristic absorption band of the carboxyl group (1718 cm^{-1}) in P(NIPAM-*co*-AA) microgels is observed in the curve of Fig. 9b, which is strong evidence of the incorporation of AA into the copolymer microgels.

3.4 Formation mechanism of the P(NIPAM-*co*-AA)/CuS composite microspheres

Based on the experimental results, the mechanism of "the deformed shrinkage of the surface texture" has been proposed.

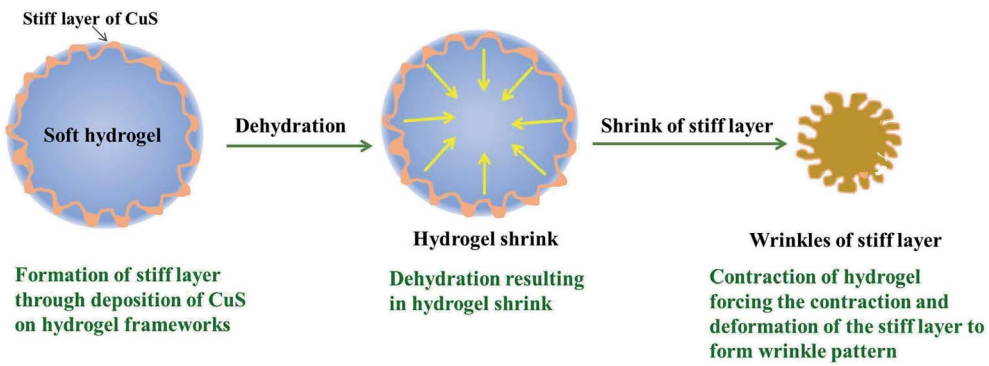

Scheme 2 The scheme of the mechanism of the composite microspheres with the wrinkle patterned surface.

© 2021 The Author(s). Published by the Royal Society of Chemistry

Open Access Article. Published on 24 November 2021. Downloaded on 2/10/2026 2:57:07 PM.
This article is licensed under a Creative Commons Attribution-NonCommercial 3.0 Unported Licence.

The above discussion is schematically represented in Scheme 2. First, the stiff layer on the soft hydrogel is formed through deposition of CuS (CuS is coming from Cu^{2+} in the hydrogel reaction with H_2S introduction) on the hydrogel frameworks. Then, dehydration of hydrogel results in the hydrogel shrinking after the P(NIPAM-*co*-AA)/CuS hydrogel was washed by acetone. Finally, the limited heterogeneity deposition of the metal sulfide on the polymeric framework of the hydrogel microspheres surface leads to the anisotropic shrinkage of the polymeric framework, and a zigzag patterned morphology on the composite microspheres surface is successfully formed. The factors affecting the deposition amount and distribution of the metal sulfide will also affect the zigzag patterned morphology. Due to the diversity of these factors (such as K_{sp}, pH, temperature, deposition amount, polymeric skeleton composition, and microgels swelling degree), the surface morphology of an appointed composite microsphere is sensitive to many factors. It revealed that even though the hydrogel and deposited metal sulfide are appointed, the surface morphology of the composite microspheres is not determined, but sensitive to reaction conditions and dehydration conditions. However, the wrinkle pattern is the result of the deformation of the metal sulfide polymer skeleton deposited on the hydrogel surface caused by the dehydration and shrinkage of the composite microspheres. In addition, the rationality of the mechanism mentioned above was confirmed from the experimental results. The morphology of the wrinkle pattern is dependent on the shrinkage degree of the hydrogel and the domain rigidity of the CuS deposition.

4. Conclusion

In conclusion, through the result of SEM images of composite microspheres under the different synthesis conditions, it has been demonstrated that the polymeric microgel clearly shows a 3D network structure, which shows that there are polymeric framework networks and rich-water domains in the swelled template of the polymeric hydrogels. Moreover, the correlation between the surface morphology of the composite microspheres and many factors affecting the metal sulfide deposition and hydrogel shrinkage were investigated. Based on the experimental results, the formation mechanism termed "the deformed shrinkage of the surface texture" was proposed, that is, the uneven deposition of the metal sulfide endows the rigid heterogeneity of the polymeric skeleton on the surface of the hydrogel. During the dehydration and contraction of the hydrogel, the surface polymeric skeleton produces an uneven deformation, thus forming the pattern morphology. This study deepens the cognition of the wrinkle pattern morphology formation.

Conflicts of interest

There are no conflicts to declare.

Acknowledgements

We gratefully acknowledge the National Science Foundation of China (21303135), the Natural Science Foundation of Shaanxi Province (2021JM-509, 2021JQ-798), the Science and Technology Program of Xi'an (21XJZZ0066), the Youth Innovation Team of Shaanxi Universities (Environmental Pollution Monitoring and Control Innovation Team, 51), and Research Team of Xi'an University (XAWLKYTD018) for financial support.

References

1 T. Chae, H. Yang, H. Moon, T. Troczynski and F. K. Ko, Biomimetically Mineralized Alginate Nanocomposite Fibers for Bone Tissue Engineering: Mechanical Properties and in Vitro Cellular Interactions, *ACS Appl. Bio Mater.*, 2020, **3**(10), 6746–6755.

2 F. C. Meldrum and H. Colfen, Controlling mineral morphologies and structures in biological and synthetic systems, *Chem. Rev.*, 2008, **108**(11), 4332–4432.

3 E. Duman, E. Ş. Kehribar, R. E. Ahan, *et al.*, Biomineralization of Calcium Phosphate Crystals Controlled by Protein−Protein Interactions, *ACS Biomater. Sci. Eng.*, 2019, **5**, 4750–4763.

4 N. Wada, N. Horiuchi, M. Nishio, *et al.*, Crystallization of Calcium Phosphate in Agar Hydrogels in the Presence of Polyacrylic Acid under Double Diffusion Conditions, *Cryst. Growth Des.*, 2017, **17**, 604–611.

5 D. Yang, L. M. Qi and J. M. Ma, Well-defined star-shaped calcite crystals formed in agarose gels, *Chem. Commun.*, 2003, **10**, 1180–1181.

6 F. Nindiyasari, L. Fernández-Díaz, E. Griesshaber, *et al.*, Influence of Gelatin Hydrogel Porosity on the Crystallization of $CaCO_3$, *Cryst. Growth Des.*, 2014, **14**(4), 1531–1542.

7 G. Vagropoulou, M. Trentsiou, A. Georgopoulou, *et al.*, Hybrid chitosan/gelatin/nanohydroxyapatite scaffolds promote odontogenic differentiation of dental pulp stem cells and in vitro biomineralization, *Dent. Mater.*, 2021, **37**(1), e23–e36.

8 M. Li, Q. Wu and J. Shi, A simple route to synthesize CuS framework with porosity, *J. Alloys Compd.*, 2010, **489**, 343–347.

9 Tengjisi, Y. Hui, G. Yang, *et al.*, Biomimetic core–shell silica nanoparticles using a dual-functional peptide, *J. Colloid Interface Sci.*, 2021, **581**, 185–194.

10 K. J. Chen, H. L. Chen and C. C. Tang, Synthesis of silica/polypeptide hybrid nanomaterials and mesoporous silica by molecular replication of sheet-like polypeptide complexes through biomimetic mineralization, *J. Colloid Interface Sci.*, 2019, **542**, 243–252.

11 S. Liu, X. Chen, Q. Zhang, W. Wu, J. Xin and J. Li, Multifunctional hydrogels based on β-cyclodextrin with both biomineralization and anti-inflammatory properties, *Carbohydr. Polym.*, 2014, **102**, 869–876.

12 G. Falini, Crystallization of calcium carbonates in biologically inspired collagenous matrices, *Int. J. Inorg. Mater.*, 2000, **2**(5), 455–461.

13 K. Huang, J. Hou, Z. Gu, *et al.*, Egg-White-/Eggshell-Based Biomimetic Hybrid Hydrogels for Bone Regeneration, *ACS Biomater. Sci. Eng.*, 2019, **5**, 5384–5391.

Open Access Article. Published on 24 November 2021. Downloaded on 2/10/2026 2:57:07 PM. This article is licensed under a Creative Commons Attribution-NonCommercial 3.0 Unported Licence.

14 A. Hernández-Gordillo, A. Hernández-Arana, A. Campero and L. Irais Vera-Robles, Biomimetic Sol−Gel Synthesis of TiO_2 and SiO_2 Nanostructures, *Langmuir*, 2014, **30**, 4084–4093.

15 B. R. Saunders and B. Vincent, Microgel particles as model colloids: theory, properties and applications, *Adv. Colloid Interface Sci.*, 1999, **80**, 1.

16 J. Bai and W.-b. Li, Simple approach to fabricate AgBr nanoparticles/polyvinylpyrrolidone microspheres, *Micro Nano Lett.*, 2010, **5**(4), 234–236.

17 J. Lv, B. Sun, J. Jin and W. Jiang, Mechanical and slow-released property of poly(acrylamide) hydrogel reinforced by diatomite, *Mater. Sci. Eng., C*, 2019, **99**, 315–321.

18 Y. Xia, Y. Gu, X. Zhou, H. Xu, X. Zhao, M. Yaseen and J. R. Lu, Controllable Stabilization of Poly(N-isopropylacrylamide)-Based Microgel Films through Biomimetic Mineralization of Calcium Carbonate, *Biomacromolecules*, 2012, **13**(8), 2299–2308.

19 S. E. Gleeson, S. Kim, Q. Qian, T. Yu, M. Marcolongo and C. Y. Li, Biomimetic Mineralization of Hierarchical Nanofiber Shish-Kebabs in a Concentrated Apatite-Forming Solution, *ACS Appl. Bio Mater.*, 2021, **4**(1), 571–580.

20 L. Wang, L. Y. Songa, Z. Y. Chao, P. P. Chen, W. Y. Nie and Y. F. Zhou, Role of surface functionality on the formation of raspberry-like polymer/silica composite particles: weak acid–base interaction and steric effect, *Appl. Surf. Sci.*, 2015, **342**, 92–100.

21 J. Yang, Y. Fang, C. Bai, D. Hu and Y. Zhang, CuS-poly (N-isopropylacrylamide-co-acrylic acid) composite microspheres with patterned surface structures: preparation and characterization, *Chin. Sci. Bull.*, 2004, **49**(19), 2026–2032.

22 Y. Fang, C. L. Bai and Y. Zhang, Preparation of metal sulfide–polymer composite microspheres with patterned surface structures, *Chem. Commun.*, 2004, 804–805.

23 J. X. Yang, D. D. Hu and Y. Fang, Novel Method for Preparation of Structural Microspheres Poly(*N*-isopropylacrylamide-*co*-acrylic acid)/SiO_2, *Chem. Mater.*, 2006, **18**, 4902–4907.

24 X. J. Wang, D. D. Hu and J. X. Yang, Synthesis of PAM/TiO_2 Composite Microspheres with Hierarchical Surface Morphologies, *Chem. Mater.*, 2007, **19**, 2610–2621.

25 J.-X. Peng, Y. Zhang, H.-Y. Xia, C.-L. Bai and Y. Fang, Studies on the Template Composition Dependence of the Surface Morphology of the Metal Sulfides-P(NIPAM-co-MAA) Composite Microspheres, *Acta Phys.-Chim. Sin.*, 2006, **22**(4), 424–429.

26 C. Bai, Y. Fang, Y. Zhang and B. Chen, Synthesis of Novel Metal Sulfide-Polymer Composite Microspheres Exhibiting Patterned Surface Structures, *Langmuir*, 2004, **20**, 263–265.

27 Y. Zhang, H. Liu, Y. Zhao and Y. Fang, Controllable synthesis of CuS–P(AM-co-MAA) composite microspheres with patterned surface structures, *J. Colloid Interface Sci.*, 2008, **325**, 391–397.

28 T. Tanaka, Kinetics of phase transition in polymer gels, *Phys. A*, 1986, **140**, 261–268.

29 A. Suzuki, S. Yoshikawa and G. Bai, Shrinking pattern and phase transition velocity of poly(N-isopropylacrylamide) gel, *J. Chem. Phys.*, 1999, **111**, 360–367.

30 T. Tanaka, S. T. Sun, Y. Hirokawa, S. Katayama, J. Kucera, Y. Hirose and T. Amiya, Mechanical instability of gels at the phase transition, *Nature*, 1987, **325**, 796–798.

31 S. Ji and J. Ding, The Wetting Process of a Dry Polymeric Hydrogel, *Polym. J.*, 2002, **34**(4), 267–270.

32 H. Li, P. Zhang, L. Zhang, T. Zhou and D. Hu, Composite microspheres with PAM microgel core and polymerisable surfactant/polyoxometalate complexes shell, *J. Mater. Chem.*, 2009, **19**, 4575–4586.

33 S. Song, S. Shen, X. Cui, D. Yao and D. Hua, Microhydrogel surface-supported quaternary ammonium peroxotungstophosphate as reusable catalytic materials for oxidation of DBT, *React. Funct. Polym.*, 2011, **71**, 512–519.

34 R. P. Washington and O. Steinbock, Frontal polymerization synthesis of temperature-sensitive hydrogels, *J. Am. Chem. Soc.*, 2001, **123**, 7933–7934.

35 E. S. Matsuo and T. Tanaka, Patterns in shrinking gels, *Nature*, 1992, **358**, 482–485.

36 S.-f. Guo, M.-q. Chen, T.-h. Lu, X.-h. Huang and M. Akashi, Spectra Studies on the Interaction of Mn^{2+} and Poly N-Isopropylacrylamide, *Spectrosc. Spectral Anal*, 2005, **25**(10), 1591–1594.

37 L. Yang, Z. Xie and Z. Li, Studied on acrylate copolymer soap-free water-borne coatings crosslinked by metal ion, *J. Appl. Polym. Sci.*, 1999, **74**(1), 91–96.

38 T. Tanaka, D. Fillmore, S.-T. Sun, I. Nishio, G. Swislow and A. Shah, Phase Transitions in Ionic Gels, *Phys. Rev. Lett.*, 1980, **45**, 1636–1639.

39 M. Ilavsky, Phase transition in swollen gels. 2. Effect of charge concentration on the collapse and mechanical behavior of polyacrylamide networks, *Macromolecules*, 1982, **15**(3), 782–788.

40 H. H. Hooper, J. P. Baker, H. W. Blanch and J. M. Prausnitz, Swelling Equilibria for Positively Ionized Polyacrylamide Hydrogels, *Macromolecules*, 1990, **23**, 1096–1104.

41 I. Ohmine and T. Tanaka, Salt effects on the phase transition of ionic gels, *J. Chem. Phys.*, 1982, **77**, 5725–5729.

42 L. Zhu, Y. Xie, X. Zheng, X. Liu and G. Zhou, Fabrication of novel urchin-like architecture and snowflake-like pattern CuS, *J. Cryst. Growth*, 2004, **260**(3–4), 494–499.

43 Y. V. Pan, R. A. Wesley, R. Luginbuhl, *et al.*, Plasma polymerized N-isopropylacrylamide: synthesis and characterization of a smart thermally responsive coating, *Biomacromolecules*, 2001, **2**(1), 32–36.

© 2021 The Author(s). Published by the Royal Society of Chemistry